

Distributed Generation Applications: Polymer Solid Oxide Fuel Cells Systems

Umesh Chandra Prasad^{1,2}, M R Prasad¹

¹ ECE Dept, Babu Banarsi Das Institute of Technology, Ghaziabad, UP

² Electrical engineering, Shri Venkateshwara University, Gajraula, Amroha, U P

Abstract - The ever-increasing need for electrical power generation, steady progress in the power deregulation and utility restructuring, and tight constraints over the construction of new transmission lines for long distance power transmission have created increased interest in distributed power generation. DG sources are normally placed close to consumption centres and are added mostly at the distribution level. They are relatively small in size and modular in structure. These DG devices can be strategically placed in power systems for grid reinforcement, reducing power losses and on-peak operating costs, improving voltage profiles and load factors, deferring or eliminating the need for system upgrades, and improving system integrity, reliability and efficiency.

The term “alternative energy” is referred to the energy produced in an environmentally friendly way (different from conventional means, i.e., through fossil-fuel power plants, nuclear power plants and hydropower plants). Alternative energy considered in this dissertation is either renewable or with high energy conversion efficiency. There is a broad range of energy sources that can be classified as alternative energy such as solar, wind, hydrogen (fuel cell), biomass, and geothermal energy. Fuel cells (FCs) are static energy conversion devices that convert the chemical energy of fuel directly into DC electrical energy. Fuel cells have a wide variety of potential applications including micro-power, auxiliary power, transportation power, stationary power for buildings and other distributed generation applications, and central power.

Fuel cell systems have high energy efficiency: The efficiency of low temperature proton exchange membrane (PEM) fuel cells is around 35-45%. High temperature solid oxide fuel cells (SOFC) can have efficiency as high as 65%. The overall efficiency of an SOFC based combined-cycle system can even reach 70%. **Renewable energy and fuel cell systems are environmental friendly:** From these systems, there is zero or low emission (of pollutant gases) that cause acid rain, urban smog and other health problems; and, therefore, there is no environmental clean-up or waste disposal cost associated with them. In this paper we should be bringing up how it is useful to make DG available using high temperature solid oxide fuel cells.

Keywords -Distributed Power Generation, Alternative Energy, Renewable energy, Polymer Electrolyte Membrane Fuel Cells, Proton Exchange Membrane, Solid Oxide Fuel Cells.

I. INTRODUCTION

In a typical fuel cell, fuel is fed continuously to the anode and oxidant is fed continuously to the cathode. The electrochemical reactions take place at the electrodes to convert chemical energy into electricity. Note that

anode is the electrode from which electrons leave (negative) and cathode is the electrode to which the electrons are coming (positive). The most common used fuel for fuel cells is hydrogen, and the oxidant is usually oxygen or air. Nevertheless, theoretically, any substance capable of chemical oxidation that can be supplied continuously (as a fluid) can be used as fuel at the anode of a fuel cell. Similarly, the oxidant can be any fluid that can be reduced at a sufficient rate.

Among different types of fuel cells, SOFC, PEMFC and MCFC are most likely to be used for distributed generation (DG) applications. Compared with conventional power plants, these Fuel Cell Distributed Generation systems have many advantages such as high efficiency, zero or low emission (of pollutant gases) and flexible modular structure. An overview is given on the operating principles of solid oxide fuel cells. SOFC is a high temperature fuel cell technology with a promising future. Based on a negative-ion conductive electrolyte, SOFCs operate between 600 C and 1000C, and convert chemical energy into electricity at high efficiency, which can reach up to 65%. The overall efficiency of an integrated SOFC-combustion turbine system can even reach 70%. Despite slow start-up and more thermal stresses due to the high operating temperature, SOFC allows for internal reforming of gaseous fuel inside the fuel cell, which gives multi-fuel capability to SOFCs. Moreover, their solid nature simplifies system designs, where the corrosion and management problems related to liquid electrolyte are eliminated. This gives SOFC a bright future to be used in stationary applications. Figure 1 shows a block diagram of a SOFC. The actions at the anode and cathode are also given in the figure 1.

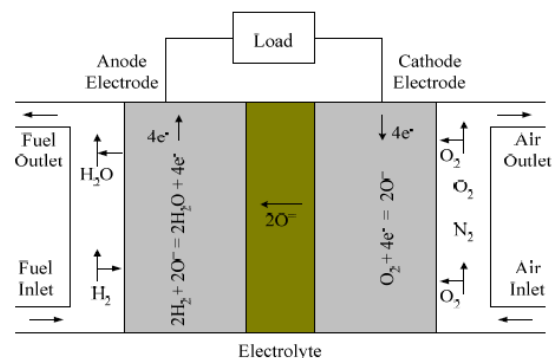


Fig 1: Schematic diagram of a SOFC.

The steady-state terminal V-I curves of a 5kW SOFC model at different temperatures, which are typical

of SOFCs, are shown in Figure 2. The activation voltage drop dominates the voltage drop in the low-current region. As load current increases, the ohmic voltage drop increases fast and becomes the main contribution to the SOFC voltage drop. When load current exceeds a certain value, fuel cell output voltage will drop sharply due to the concentration voltage drop inside SOFC. Figure 2 also shows the effect of temperature on SOFC V-I characteristic curve. SOFC output voltage is higher at lower temperature in the low current zone while the voltage is higher at higher temperature in the high current region.

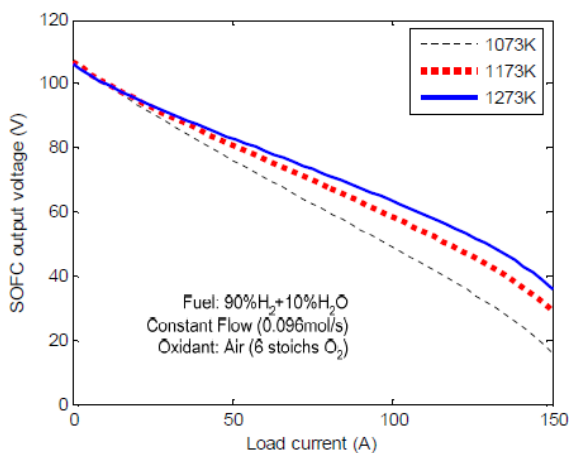


Fig 2: V-I characteristic of a 5kW SOFC stack

II. DYNAMIC MODELS FOR SOFC

Solid oxide fuel cells are advanced electrochemical energy conversion devices operating at a high temperature, converting the chemical energy of fuel into electric energy at high efficiency. They have many advantages over conventional power plants and show great promise in stationary power generation applications. The energy conversion efficiency of a SOFC stack can reach up to 65%, and its overall efficiency, when used in combined heat and power (CHP) applications, i.e., as an integrated SOFC-combustion turbine system, can even reach 70%. Despite slow start-up and thermal stresses due to the high operating temperature, SOFC allows for internal reforming of gaseous fuel inside the fuel cell, which gives its multi-fuel capability. SOFC modelling is of interest for its performance prediction and controller design. Many SOFC models have been developed; some are highly theoretical and are based on empirical equations, and some are more application oriented. Increased interest in SOFC power plant design and control has led to a need for appropriate application oriented SOFC models. An integrated SOFC plant dynamic model for power system simulation (PSS) software with three operation limits of SOFC power plants were addressed in paper in order to achieve a safe and durable cell operation. However, the thermodynamic properties of SOFCs were not discussed in this paper. A transient model of a tubular SOFC consisting of an

electrochemical model and a thermal model is given. However, the dynamic response of the model due to load variations was only investigated in large (minute) time scale. A dynamic model of a tubular SOFC stack is presented based on its thermodynamics and electrochemical properties, and on the mass and energy conservation laws, with emphasis on the fuel cell electrical (terminal) characteristics.

The SOFC model, implemented in MATLAB/Simulink®, mainly consists of an electrochemical sub-model and a thermodynamic sub-model. The double-layer charging effect is also taken into account in the model. The model responses are studied under both constant fuel flow and constant fuel utilization operating modes. The effect of temperature on the steady-state V-I (output voltage vs. current) and P-I (output power vs. current) characteristics are also studied. The dynamic responses of the model are given and discussed in different time scales, i.e., from small time scale (10^{-3} - 10^1 s) to large time scale (10^2 - 10^3 s). The temperature response of the model is given as well. The SOFC model has been used to study the SOFC overloading capability and to investigate the performance of a SOFC distributed generation system. The model shows the potential to be useful in SOFC related studies such as real-time control of SOFC and its distributed generation applications.

A. Dynamic Model Development

A mathematical approach is presented for building a dynamic model for a tubular SOFC fuel cell stack. To simplify the analysis, the following assumptions are made:

- One-dimensional treatment.
- $O=$ conducting electrolytes and ideal gases.
- H_2 fuel and large stoichiometric quantity of O_2 at cathode.
- H_2 and O_2 partial pressure are uniformly decreased along the anode channel while the water vapor partial pressure is uniformly increased for normal operations.
- Lumped thermal capacitance is used in the thermodynamic analysis, and the effective temperature of flowing gases in gas channels (anode and cathode channels) is represented by its arithmetical mean value, $T_{ch\ gas} = (T_{in\ gas} - T_{out\ gas})/2$.
- The combustion zone is not model in this SOFC thermal model. The fuel and air are assumed to be pre-heated.
- Parameters for individual cells can be lumped together to represent a fuel cell stack.

A schematic diagram of a SOFC is shown in Figure 3. Two porous electrodes (anode and cathode) are separated by a solid ceramic electrolyte. This electrolyte material (normally dense yttria-stabilized zirconia) is an excellent conductor for negatively charged ions (such as $O=$) at high temperatures. At the cathode, oxygen molecules accept electrons from the external circuit and change to oxygen ions. These negative ions pass across the

electrolyte and combine with hydrogen, at the anode, to produce water.

Effective Partial Pressures - In this part, expressions for H_2 , O_2 and H_2O partial pressures at anode and cathode channels and their effective values at actual reaction sites are derived in terms of the fuel cell operating parameters (e.g., fuel cell temperature, fuel and oxidant flow rates, and anode and cathode inlet pressures) and the physical and electrochemical parameters of the fuel cell. These partial pressure values will be used to calculate the fuel cell output voltage.

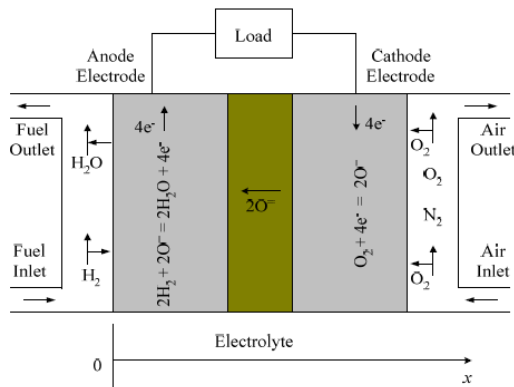


Fig 3: Schematic diagram of a solid oxide fuel cell

As shown in above Figure 3, when load current is being drawn, H_2 and O_2 will diffuse through the porous electrodes to reach the reaction sites, and the reactant H_2O will diffuse from the reaction sites to the anode channel. As a result, H_2 , H_2O and O_2 partial pressure gradients will be formed along the anode and cathode channels when the fuel cell is under load. Assuming uniform variation of gas partial pressures, the arithmetic mean values are used to present the overall effective gas partial pressures in the effective partial pressures of H_2 and O_2 at the actual reaction sites will be less than those in the gas flow channels due to mass diffusion. In contrast, the vapor partial pressure at reaction sites is higher than that in the anode flow channel. In order to calculate the fuel cell output voltage, the effective partial pressures of H_2 , H_2O and O_2 at the reaction sites need to be determined. In a gas mixture consisting of N species, the diffusion of component i through the porous electrodes can be described by the Stefan-Maxwell formulation:

$$\nabla x_i = \frac{RT}{P} \sum_{j=1}^N \frac{x_i N_j - x_j N_i}{D_{i,j}}$$

Where; x_i (x_j) = Mole fractions of species i (j);
 $D_{i,j}$ = effective binary diffusivity of i - j pair (m^2/s);
 N_i (N_j) = Superficial gas flux of species i (j) [$mol/(m^2 \cdot s)$];
 R = gas constant, $8.3143 \text{ J/(mol} \cdot \text{K)}$;
 T = gas temperature (K);
 P = overall pressure of the gas mixture (Pa).

In the anode channel, the gas stream is a mixture of H_2 and H_2O . In the one-dimensional transport process along the x axis, shown in Figure 3 the diffusion of H_2 can be simplified theoretically and the activation voltage drop will be zero when load current is zero. The ohmic and concentration voltage drops are also zero when the fuel cell is not loaded ($i=0$). However, even the open-circuit voltage of a SOFC is known to be less than the theoretical value given.

Ohmic Voltage Drop- The ohmic resistance of a SOFC consists mainly of the resistance of the electrolyte, electrodes and interconnection between fuel cells. In this model, only ohmic losses of electrolyte and interconnection are included while the resistance of electrodes is neglected.

Concentration Voltage Drop- During the reaction process, concentration gradients can be formed due to mass diffusion from the flow channels to the reaction sites (catalyst surfaces). The effective partial pressures of hydrogen and oxygen at the reaction site are less than those in the electrode channels, while the effective partial pressure of water at the reaction site is higher than that in the anode channel. At high current densities, slow transportation of reactants (products) to (from) the reaction site is the main reason for the concentration voltage drop.

Double-layer charging effect - In a SOFC, the two electrodes are separated by the electrolyte (Figure 3) and two boundary layers are formed, e.g. anode-electrolyte layer and electrolyte-cathode layer. These layers can be charged by polarization effect, known as electrochemical double-layer charging effect, during normal fuel cell operation. The layers can store electrical energy and behave like a super-capacitor. The model for SOFC considering this effect can be described by the equivalent circuit shown in Figure 4.

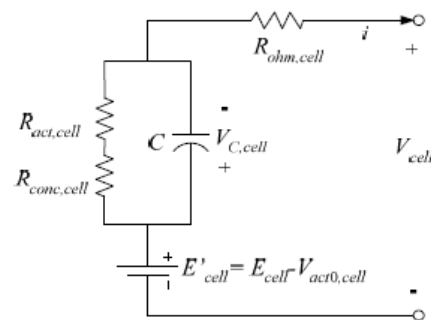


Fig 4: Equivalent electrical circuit of the double-layer charging effect inside a SOFC.

In the above circuit, $R_{ohm,cell}$, $R_{act,cell}$ and $R_{conc,cell}$ are equivalent resistances of ohmic voltage drop, activation and concentration voltage drops, which can be calculated. C is the equivalent capacitance of the double-layer charging effect. Since the electrodes of a SOFC are

porous, the value of C is large and can be in the order of several Farads. The voltage across C can be calculated to find the output voltage, V_{out} , of a SOFC stack.

Energy Balance of the Thermodynamics- The cross section profile and heat transfer inside a tubular SOFC are shown in Figure 5. One advantage of this tubular structure is that it eliminates the seal problems between cells since the support tube of each cell is closed at one end. The air is fed through a central air supply tube (AST) and forced to flow back past the interior of the cell (cathode surface) to the open end. The fuel gas flows past the exterior of the cell (anode surface) and in parallel direction to the air. The thermal analysis for fuel reformer and combustor are not included in this model. Heat exchanges between cells are also not considered in this model by assuming that temperature differences between adjacent cells can be neglected. Heat transport inside the fuel cell occurs mainly by means of radiation, convection and mass flow.

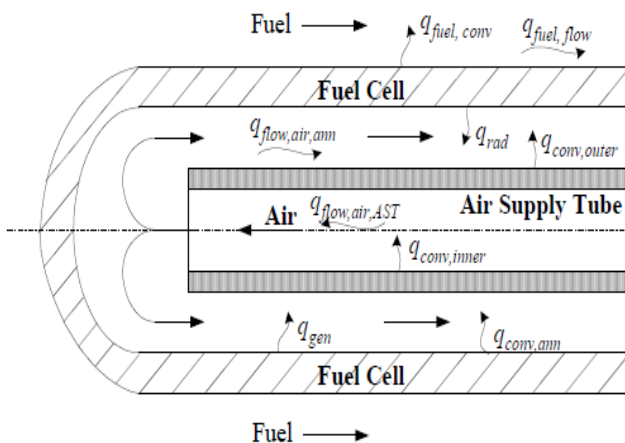


Fig 5: Heat Transfer inside a tubular solid oxide fuel cell.

B. Dynamic SOFC Model Implementation

A dynamic model for a 5kW SOFC has been developed in MATLAB/Simulink, based on the electrochemical and thermodynamic characteristics of the fuel cell discussed in the previous section. The output voltage of the fuel cell depends on conditions including fuel composition, fuel flow, oxidant flow, anode and cathode pressures, cell temperature, load current and the electrical and thermal properties of the cell materials. Figure 6 shows the block diagram, based on which the model has been developed. In this figure, the input quantities are anode and cathode pressures (P_a and P_c), H_2 flow rate (M_{H_2}), H_2O flow rate (M_{H_2O}), air flow rate (M_{air}) and initial temperature of the fuel cell and air ($T_{fuelinlet}$ and $T_{airinlet}$). At any given load current and time, the cell temperature T_{cell} is determined and both the load current and temperature are fed back to different blocks, which take part in the calculation of the fuel cell output voltage. In this block diagram, material conservation equations are used to calculate the partial pressures of H_2 , H_2O and O_2 in flow channels. Then, the Nernst equation is employed to determine the internal potential (E) of the

fuel cell. Diffusion equations and the material conservation equations will give the concentration loss of the cell. The ohmic voltage drop and activation voltage is computed. Eventually, the terminal (output) voltage of the fuel cell and the double-layer charging effect are calculated. The thermal model is developed via energy balance equations (4 Model Responses under Constant Fuel Flow Operation Both the steady-state and dynamic responses of the SOFC model under constant flow operating mode are given). The thermodynamic response of the model and the impact of the operating temperature are also given. The dynamic responses of the model are investigated in different time scales.

C. Model Responses under Constant Fuel Flow Operation

Both the steady-state and dynamic responses of the SOFC model under constant flow operating mode are given in this section. The thermodynamic response of the model and the impact of the operating temperature are also given. The dynamic responses of the model are investigated in different time scales.

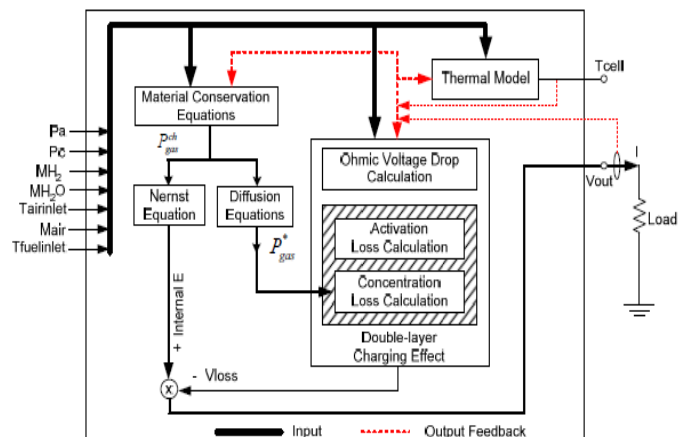


Fig 6: Diagram of building a dynamic model of SOFC in SIMULINK.

The steady-state terminal voltage vs. current (V-I) curves of the SOFC model at different temperatures are shown in Figure 7. These curves are similar to the real test data reported in. The activation voltage drop dominates the voltage drop in the low-current region. As load current increases, the ohmic voltage drop increases fast and becomes the main contribution to the SOFC voltage drop. When the load current exceeds a certain value (140A for this SOFC model) the fuel cell output voltage will drop sharply due to large ohmic and concentration voltage drops inside SOFC. The variations of the above three voltage drops vs. load current at three different temperatures are shown in Figure 8. Figure 7 shows the effect of temperature on the SOFC V-I characteristic curve. The SOFC output voltage is higher at lower temperature in the low current zone while the voltage is higher at higher temperature in the high current region. These simulation results showing the effect of temperature on SOFC performance are also similar to the test data. The negative temperature coefficient of the open-circuit

internal potential E_{0cell} , and the temperature-dependent activation voltage drop and ohmic voltage drop (shown in Figure 8) are the main reasons for this kind of temperature dependent performance of the SOFC model. As shown in Figure 8, both the activation and ohmic voltage drops decrease as the fuel cell temperature increases.

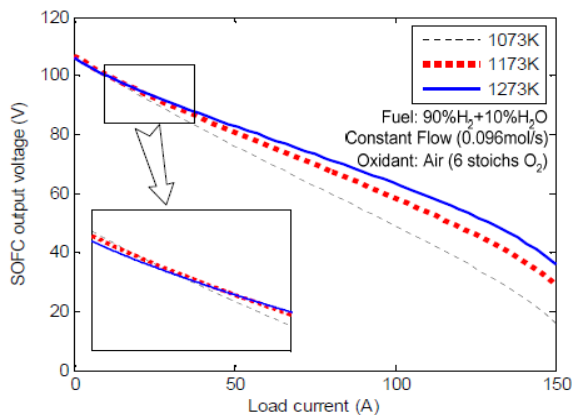


Fig 7: V-I characteristics of the SOFC model at different temperatures.

The corresponding output power vs. current (P-I) curves of the model at different temperatures are shown in Figure 4.22. At higher load currents ($I > 40$ A), higher output power can be achieved at higher operating temperatures. Under each operating temperature, there is a critical load current point (I_{crit}) where the model output power reaches its maximum value. For example, I_{crit} is 95 A at 1073 K, 110 A at 1173 K and 120 A at 1273 K. Beyond these points, an increase in the load current will reduce the output power due to large ohmic and concentration voltage drops.

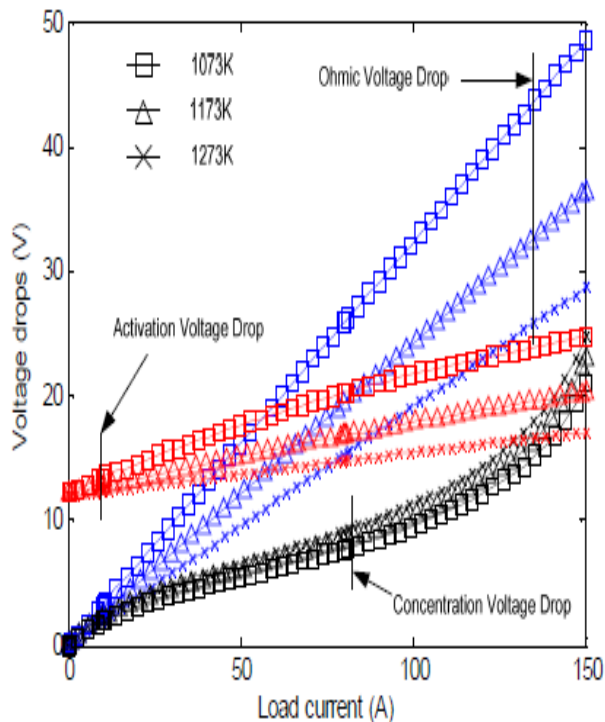


Fig 8: Three voltage drops at different temperatures.

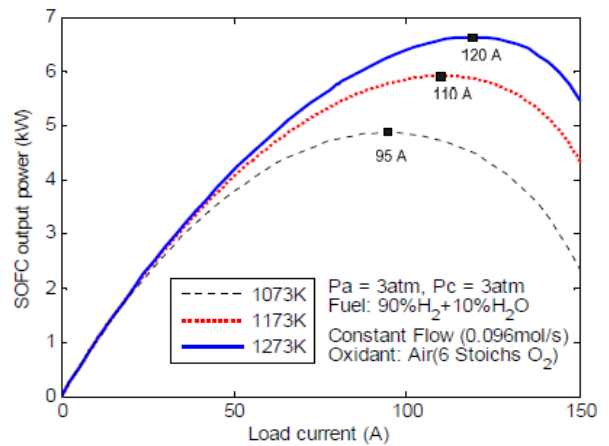


Fig 9: P-I characteristics of the SOFC model at different temperatures

Dynamic Response- The dynamic response of the SOFC model is mainly dominated by the double-layer charging effect, the time constants G_a and G_c , and the thermodynamic property of the fuel cell. Although the capacitance (C) of the double-layer charging effect is large (in the order of several Farads), the time constant $G_{dlc} = (R_{act,cell} + R_{conc,cell})C$ is normally small (in the order of around 10-2 s) because $(R_{act,cell} + R_{conc,cell})$ is small (less than 2.0 m Ω for a single cell used in this study) when the fuel cell works in the linear zone. Therefore, capacitor C will only affect the model dynamic response in small time scale, i.e., 10^{-3} - 10^{-1} s. The operating conditions of the SOFC model for this simulation study are listed in Table 1. Figure 10 shows the model dynamic responses in this small time scale under step current changes. The load current steps up from 0 A to 80 A at 0.1 s and then steps down to 30 A at 0.2 s. The lower part of the figure shows the corresponding SOFC output voltage responses with different capacitance values for the double-layer charging effect. When the load current steps up (down), the fuel cell output voltage drops (rises up) immediately due to the ohmic voltage drop. Then the voltage drops (rises) "smoothly" to its final value. It is noted that the larger is the capacitance C , the slower the output voltage reaches its final value because the larger is the effective time constant G_{dlc} .

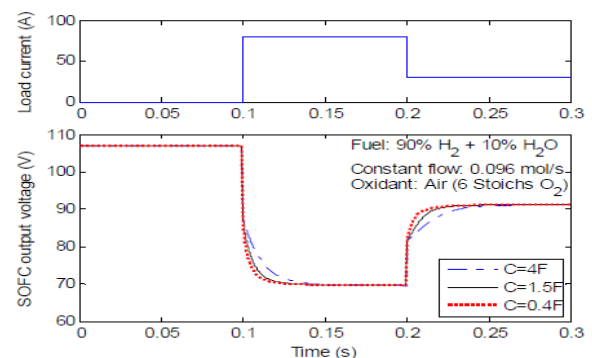


Fig 10: Model dynamic responses with different equivalent capacitance values for double-layer charging effect in small time scale.

TABLE 1 OPERATING CONDITIONS FOR THE MODEL DYNAMIC RESPONSE STUDIES

Temperature (K)	1173
Anode input pressure (atm)	3
Cathode input pressure (atm)	3
Anode H ₂ flow rate (mol/s)	0.0864
Anode H ₂ O flow rate (mol/s)	0.0096
Oxidant	Air (6 stoichs O ₂)

Time constants G_a and G_c are in the order of 10-1-100 s for the model parameters used in this dissertation. They mainly affect the model dynamic responses in the time scale 10-1 to 101 s. Figure 11 shows the model dynamic responses in this medium time scale under the same type of step current changes as shown in Figure 10. The load current steps up from 0 A to 80 A at 1s and then steps down to 30 A at 11s. The operating conditions of the model are the same as given in Table 1 except for the operating pressures. Figure 11 shows the SOFC output voltage responses under different operating pressures ($P_a = P_c = P$). Higher operating pressure gives higher output voltage and also increases time constants G_a and G_c , shown in the figure.

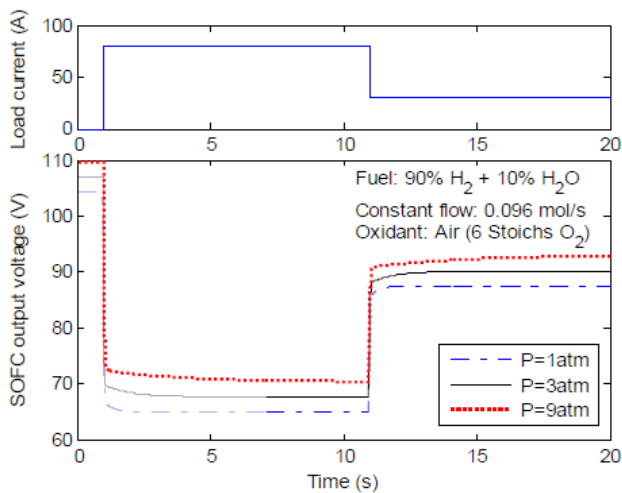


Fig 11: Model dynamic responses under different operating pressures in medium time scale.

The equivalent thermodynamic time constant of a SOFC can be in the order of tens of minutes. Thus, for a large time scale (102-103 s), the thermodynamic characteristic will dominate the model dynamic responses. Figure 12 shows the transient response of the SOFC model under load changes. The model was subjected to a step change in the load current from zero to 100 A at 10 min and then the current drops back to 30 A at 120 min. The operating conditions are also the same as given in Table 4.4 except for the varying fuel cell operating temperatures. The fuel and air inlet temperatures are given in the figure. When the load current steps up, the SOFC output voltage drops sharply, and then rises to its final value. When the load current steps down, the output voltage jumps up and then drops slowly towards its final value, as shown in Figure 12.

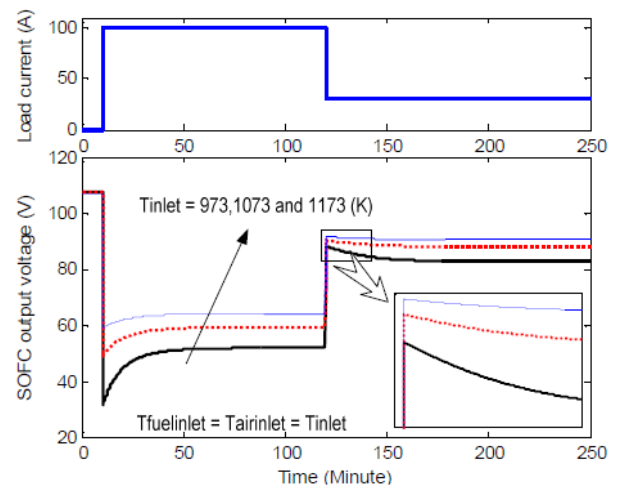


Fig 12: Model dynamic responses under different inlet temperatures in large timescale.

The corresponding temperature responses of the SOFC model are shown in Figure. From this figure, the equivalent overall thermodynamic time constant of the model is around 15 minutes.

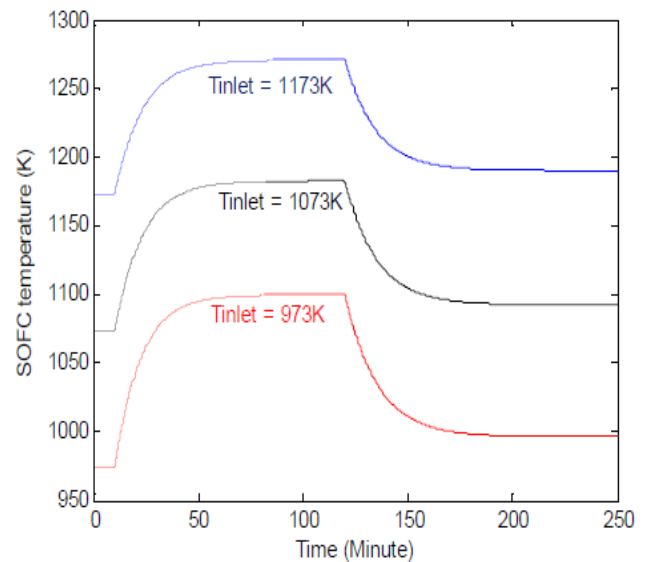


Fig 13: Model temperature responses.

D. Constant Fuel Utilization Operation

The fuel cell can also be operated in constant fuel utilization mode, in which the utilization factor will be kept constant. The direct way to achieve constant utilization operation is to feed back the load current with a proportional gain $1/(2F_{xu})$, as shown in Figure 13, to control fuel flow to the fuel processor. As a result, the input H₂ will change as load varies to keep the fuel utilization constant. As shown in Figure 14, the fuel processor is modelled by a simple delay transfer function is set to 5s in this research.

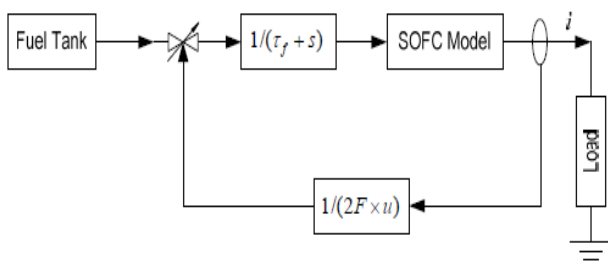


Fig 14: Constant utilization control.

The fuel cell's steady state- characteristics and dynamic responses under constant fuel utilization mode will be discussed. The results will also be compared with those obtained under constant flow operating mode. The utilization factor is set for 0.85 (85% fuel utilization) for this study and other operating conditions are the same as listed in Table1 except the fuel and water flow rates that will change as the load current changes.

Steady-state Characteristics- Figure 15 shows a comparison between the V-I characteristic of the SOFC model with constant fuel utilization and constant fuel flow operating modes. The operating conditions for the constant flow operating mode are listed in Table1. For this specific study, the output voltage under constant flow operating mode is higher than that under constant utilization mode at the same load current. The voltage difference between the two operating modes keeps getting smaller as the load current increases. The reason for this is that the utilization factor of the constant flow operation will be getting closer to the utilization factor (0.85) of the constant utilization operation as load current increases. The corresponding P-I curves, also given in Figure 15, show that the SOFC can provide more power under constant flow operation.

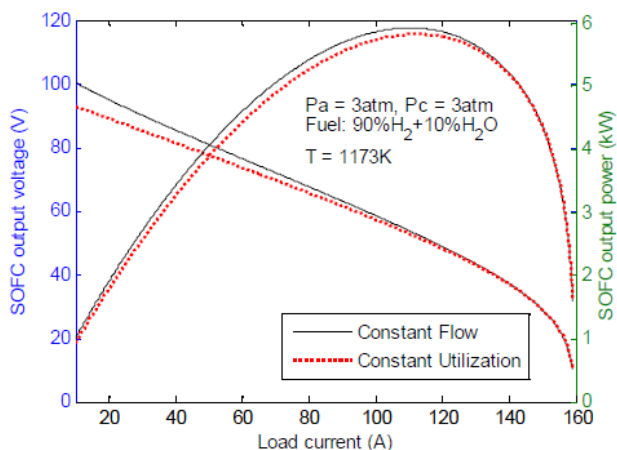
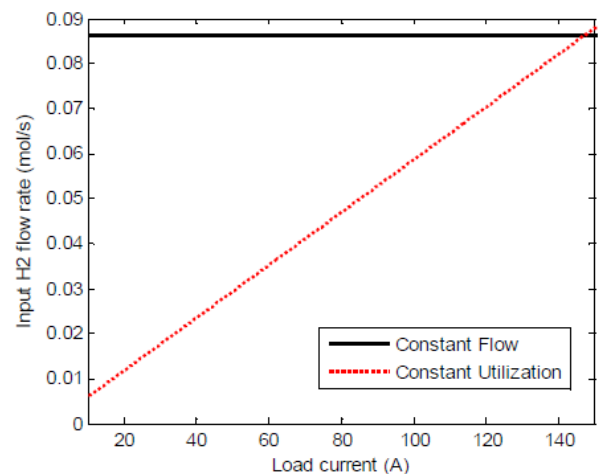


Fig 15: V-I and P-I characteristics of the SOFC model under constant fuel utilization and constant fuel flow operating modes.

Figure 16 shows the curves of input fuel versus load current for both operation modes. It shows that the constant flow operation mode requires more fuel input, especially at light loading. But the unused H₂ is not just wasted; it can be used for other purposes or recycled to use again.

Fig 16: H₂ input for the constant utilization and constant flow operating modes.

Dynamic response of the SOFC model- In small time scale is dominated by the double-layer charging effect and in large time scale is mainly determined by the thermodynamic properties of the fuel cell. Both the double-layer charging effect and the thermodynamic characteristics of the fuel cell are determined by the fuel cell's physical and electrochemical properties. These properties are normally not affected by whether the SOFC is operating under constant fuel flow mode or constant fuel utilization mode. However, the dynamic response in medium time scale will be affected by the operating mode since the fuel flow rate will change as load varies under constant utilization operating mode. This load-dependent fuel flow rate will give a load-dependent time constant τ_a as well. Therefore, only the dynamic response in this time scale will be discussed for the constant utilization operating mode.

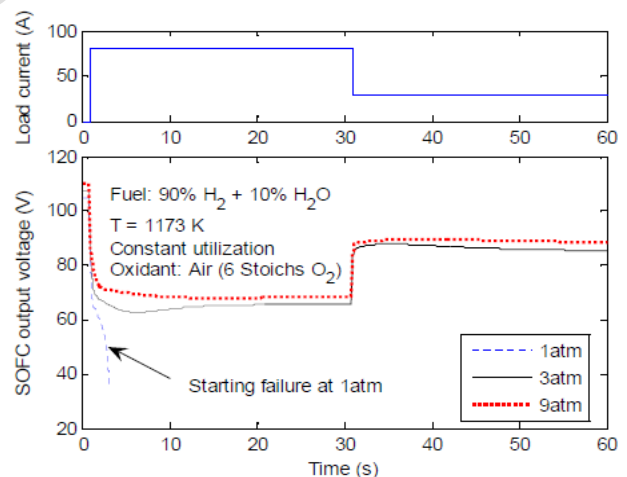


Fig 17: Model dynamic responses under different operating pressures in the medium time scale with constant utilization operating mode

Figure 17 shows the model dynamic responses in the medium time scale under similar step current changes used in the constant fuel flow operating mode. The load current steps up from 0 A to 80 A at 1s and then steps down to 30 A at 31 s. The lower part of Figure 17 shows the corresponding SOFC output voltage responses under

different operating pressures. Similar to what is shown in Figure 11 for constant fuel flow operating mode, a higher operating pressure results in a higher output voltage and larger time constants G_a and G_c . In this case, the dynamic responses are not determined only by G_a and G_c , but also by the dynamics of the fuel processor. The output voltage curves (Figure 17) show the typical characteristic of a second order system while the dynamic responses in medium time scale for the constant flow operating mode (Figure 11) exhibit the characteristic of a first order system. Figure 17 shows that the SOFC output voltage drops as the load current steps up, undershoots, and then rises back to its final value. While the load current steps down, the voltage rises up, overshoots, and then drops back to its final value. It is noted that the fuel cell fails to start up at 1 atmospheric operating pressure due to the delay in the fuel processor, which causes insufficient fuel supply.

III. CONCLUSIONS

For a SOFC array, its configuration can be determined in a similar way. According to the SOFC V-I and P-I characteristics, when its load current is over 110 A, the SOFC stack is in the concentration zone, where its output voltage will decrease sharply as load current increases. In order to leave some safe margin, the fuel cell is operated around the point where its current is 100 A (rated operating point), and its output voltage (V_{SOFC}) is about 55 V. Therefore, the number (N_s) of fuel cell stacks we need to connect in series to get a voltage of 220 V is 4.

The total power rating of the series connection of 4 SOFC stacks (5 kW each) is 20 kW. The number (N_p) of these 20 kW SOFC units that need to be connected in parallel to compose a 40 kW fuel cell array is 8 SOFC stacks (5 kW each). Super-capacitors or battery banks are connected to the DC bus to provide storage capability and fast dynamic response to load transients. A 3-phase 6-switch inverter interfaces the DC bus with a 120/220 V AC power system. An LC filter is connected to the output of the inverter to reduce the harmonics introduced by the inverter. A 220V/12.5kV step up transformer connects the fuel cell power system to the utility grid through a coupling inductor and a short transmission line. The coupling inductor is needed to control the real and reactive power flow between the fuel cell DG system and the utility grid and to limit disturbance and fault currents. The controllers for the boost DC/DC converters are designed to keep the DC bus voltage within an acceptable band ($\pm 5\%$ in this study). Therefore, the input to the 3-phase inverter can be considered as a fairly good constant voltage source. The inverter controller controls the real and reactive power flows to the utility grid. P, Q power flows follow their respective reference values, which can either be set as fixed values or to follow a certain load demand.

In SOFC DG, The output voltage and current curves of each 40 kW SOFC array (input to each DC/DC converter) for the above heavy loading, when the system output power reaches its pre-set value, the fuel cell output current

ripple is about 10% and the fuel cell output voltage ripple is around 3%. These relatively small variations of the current and voltage are indicative of the healthy operation of fuel cells. The DC bus voltage (output voltage of the boost DC/DC converter) is the DC bus voltage comes up to its reference value (480V) though the fuel cell terminal voltage is much lower than its no-load value under this heavy loading condition. The voltage ripple at the DC bus is about 1.5%, which is within the acceptable range.

REFERENCES

- [1] Archie W. Culp, Jr., (1979), Principles of Energy Conversion, McGraw-Hill Book Company.
- [2] J. Hatziaioniu, A.A. Lobo, F. Pourboghraat and M. Daneshdoost, "A simplified dynamic model of grid-connected fuel-cell generators," IEEE Transactions on Power Delivery, Vol. 17, No. 2, pp. 467-473, April 2002.
- [3] Wang, M.H. Nehrir, and S.R. Shaw, "Dynamic Models and Model Validation for PEM Fuel Cells Using Electrical Circuits," IEEE Transactions on Energy Conversion, Vol. 20, No. 2, pp.442-451, June 2005.
- [4] L. Harder, (1982), Fundamentals of Energy Production, John Wiley & Sons.
- [5] E.R.G. Eckert and R. M. Drake, Jr., (1972), Analysis of Heat and Mass Transfer, McGraw-Hill Book Company.
- [6] F.A. Farret and M.G. Simões, (2006), Integration of Alternative Sources of Energy, John Wiley & Sons, Inc.
- [7] F.T. Ulaby, (1999), Fundamentals of Applied Electromagnetics, Prentice-Hall, Inc.
- [8] G. Hoogers, (2003), Fuel Cell Technology Handbook, CRC Press LLC.
- [9] George N. Hatsopoulos and Joseph H. Keenan, (1965), Principles of General Thermodynamics, John Wiley & Sons Inc.
- [10] Hubertus P.L.H. van Bussel, Frans G.H. Koene and Ronald K.A.M. Mallant, "Dynamic Model of Solid Polymer Fuel Cell Water Management," Journal of Power Sources, Vol. 71, No. 1-2, pp. 218-222, March 1998.
- [11] J. C. Amphlett, R. M. Baumert, R. F. Mann, B. A. Peppley and P. R. Roberge, "Performance Modeling of the Ballard Mark IV Solid Polymer Electrolyte Fuel Cell, II. Empirical Model Development," Journal of the Electrochemical Society, Vol. 142, No. 1, pp. 9-15, Jan. 1995.
- [12] J. Padullés, G.W. Ault, and J. R. McDonald, "An integrated SOFC plant dynamic model for power system simulation," J. Power Sources, pp.495-500, 2000.
- [13] James Larminie and Andrew Dicks, (2001), Fuel Cell Systems Explained, John Wiley & Sons, Ltd..
- [14] K. Eguchi, H. Kojo, T. Takeguchi, R. Kikuchi and K. Sasaki, "Fuel flexibility in power generation by solid oxide fuel cells," Solid State Ionics, No. 152-153: pp. 411-16, Dec. 2002.
- [15] K. Sedghisigarchi and A. Feliachi, "Dynamic and Transient Analysis of Power Distribution Systems with Fuel Cells—Part I: Fuel-Cell Dynamic Model," IEEE Transactions on Energy Conversion, Vol. 19, No. 2, pp.423-428, June 2004.
- [16] K. Sedghisigarchi and A. Feliachi, "Dynamic and Transient Analysis of Power Distribution Systems with Fuel Cells—Part II: Control and Stability Enhancement," IEEE Transactions on Energy Conversion, Vol. 19, No. 2, pp.429-434, June 2004.
- [17] O. Yamamoto, "Solid oxide fuel cells: fundamental aspects and prospects," Electrochimica Acta, Vol. 45, No. (1516), pp. 2423-2435, 2000.
- [18] P. Aguiar, D. Chadwick and L. Kershenbaum, "Modeling of an indirect internal reforming solid oxide fuel cell," Chemical Engineering Science, Vol. 57, pp.1665-1677, 2002.
- [19] P. Costamagna and K. Honegger, "Modeling of solid oxide heat exchanger integrated stacks and simulation at high fuel utilization," Journal of the Electrochemical Society, Vol. 145, No. 11, pp. 3995-4007, Nov. 1998.
- [20] R. Cownden, M. Nahon, M. A. Rosen, "Modeling and Analysis of a Solid Polymer Fuel Cell System for Transportation Applications," International Journal of Hydrogen Energy, Vol. 26, No. 6, pp. 615-623, June 2001.

- [21] R.S. Gemmen, "Analysis for the effect of inverter ripple current on fuel cell operating condition," Transactions of the ASME - Journal of Fluids Engineering, Vol. 125, No. 3, pp.576-585, May 2003.
- [22] S. H. Chan, C.F. Low, O.L. Ding, "Energy and exergy analysis of simple solid-oxide fuel-cell power systems," Journal of Power Sources, Vol. 103, No.2, pp. 188-200, Jan. 2002.
- [23] S.C. Singhal, "Solid oxide fuel cells for stationary, mobile and military applications," Solid State Ionics, Vol. 152-153, pp.405-410, 2002.
- [24] S.H. Chan, K.A. Khor and Z.T. Xia, "A complete polarization model of a solid oxide fuel cell and its sensitivity to the change of cell component thickness," Journal of Power Sources, Vol. 93, No. (1-2), pp. 130-140, Feb 2001.
- [25] Steven S. Zumdahl, (1995), Chemical Principles, 2nd Edition, DC Heath and Company, Toronto.
- [26] Z. Miao, M. A. Choudhry, R. L. Klein and L. Fan, "Study of A Fuel Cell Power Plant in Power Distribution System – Part I: Dynamic Model," Proc. IEEE PES General Meeting, Denver, CO, June 2004.



Umesh Chandra Prasad completed his B. Tech from BIT, Ranchi University and was commissioned as an Air Force Officer, where he served the nation for 29 years in various capacities, being an Aeronautical Engineer (Electronics). During his tenure, he completed

M.Tech degree from IIT Delhi in Systems. He also worked as an Instructor with Air Force Technical College and other Institutes of IAF. Further, He did Executive Management from MDI Gurgaon. After his retirement, he was working as the Director- Academics with an Engineering and Management Institute. He has recently completed his PhD from IIT Delhi. He is also a fellow of Institutions of Engineers (India) and IETE.